NAVAL POSTGRADUATE SCHOOL
Monterey, California

THESIS

FINITE-AMPLITUDE STANDING WAVES

IN A RIGID WALLED CAVITY

by

Christopher "K" Lane

Thesis Advisor: Alan B. Coppens

June 1972

Approved for public release; distribution unlimited.

Unclassified

Security Classification

DOCUMENT CONTROL DATA - R & D

(Security classification of title, body of abstract and indexing annotation must be entered when the overall report is classified)

1. ORIGINATING ACTIVITY (Corporate author)	2a. REPORT SECURITY CLASSIFICATION
Naval Postgraduate School Monterey, California 93940	Unclassified
	2b. GROUP

3. REPORT TITLE

Finite-Amplitude Standing Waves in a Rigid Walled Cavity

4. DESCRIPTIVE NOTES *(Type of report and, inclusive dates)*

Master's Thesis; June 1972

5. AUTHOR(S) *(First name, middle initial, last name)*

Christopher "K" Lane

6. REPORT DATE	7a. TOTAL NO. OF PAGES	7b. NO. OF REFS
June 1972	43	18

8a. CONTRACT OR GRANT NO.	9a. ORIGINATOR'S REPORT NUMBER(S)
b. PROJECT NO.	
c.	9b. OTHER REPORT NO(S) *(Any other numbers that may be assigned this report)*
d.	

10. DISTRIBUTION STATEMENT

Approved for public release; distribution unlimited.

11. SUPPLEMENTARY NOTES	12. SPONSORING MILITARY ACTIVITY
	Naval Postgraduate School Monterey, California 93940

13. ABSTRACT

Finite-amplitude standing waves in air at ambient temperature contained in a rigid-walled rectangular cavity were experimentally investigated. The pressure waveform in the cavity was analyzed for harmonic content and compared to the theory of Coppens and Sanders as modified to include empirical losses. The waveforms for the n00 and 0n0 configurations were analyzed at strength parameters of about 0.5, 0.75, and 1.0, where the strength parameter is defined as $MQ_1(\gamma + 1)/2$. M is the Mach number of the fundamental, Q_1 is the quality factor of the fundamental resonance, and γ is the ratio of specific heats. It is found that the theoretical model accurately predicts the shape and approximates the amplitudes of the harmonic components of the finite-amplitude standing waves.

DD FORM 1 NOV 68 1473 (PAGE 1)

S/N 0101-807-6811

Unclassified

Security Classification

14. KEY WORDS	LINK A		LINK B		LINK C	
	ROLE	WT	ROLE	WT	ROLE	WT
Finite-amplitude standing waves						
Rigid-walled cavity						
Strength parameter						
Frequency parameter						
Perturbation approach						
Fourier synthesis approach						

Finite-Amplitude Standing Waves

In a Rigid-Walled Cavity

by

Christopher "K" Lane
Ensign, United States Navy
B.S., Oregon State University 1971

Submitted in partial fulfillment of the
requirements for the degree of

MASTER OF SCIENCE IN PHYSICS

from the

NAVAL POSTGRADUATE SCHOOL
June 1972

Author Christopher K Lane

Approved by: Allan B. Coppens
Thesis Advisor

Otto Heinz
Chairman, Department of Physics

Academic Dean

TABLE OF CONTENTS

ACKNOWLEDGEMENT

The encouragement and advice of Professor Alan B. Coppens is gratefully acknowledged.

Thanks are also due Mr. Robert C. Moeller for his assistance in fabricating the apparatus.

I. INTRODUCTION

The purpose of this research is to make a detailed investigation of finite-amplitude standing waves in air at ambient temperatures in a rigid walled cavity, for comparison with the theory of Coppens and Sanders [1] modified to include observed energy losses. This investigation is a continuation of the experimental works of Beech [2] and Winn [3], with an extension to a rectangular cavity vice a long round tube.

A rectangular cavity was chosen as it was a step toward the study of two and three dimensional waves, although this investigation concerns only one dimensional standing waves. In addition, it was thought that a rectangular geometry would produce overtones which would be less harmonic than those for the more symmetric geometry of the round tube. The dimensions of the cavity were chosen in an effort to space out the system resonances to avoid degeneracy or near-degeneracy. This was accomplished with some success, and thus allowed for the accurate location and analysis of the first few overtones of each of the two modes studied.

II. BACKGROUND AND THEORY

A finite amplitude wave is a solution of the non-linear wave equation that describes the real-life environment that confronts large amplitude acoustic waves. This finite-amplitude wave requires second order terms, or higher, to describe the waveform.

It has been known for many years that hydrodynamic equations describing traveling waves in a non-dissipative medium predict a change in the waveform. Kirchoff [4] and Lamb [5] were among the early investigators in this area. In more recent years there have been many theories and methods of solution proposed to describe this distorted traveling waveform in a non-dissipative medium. Amoung these are the works of Fay [6], and Blackstock [7] who produced an extensive theoretical treatment of low amplitude non-linear waves, and made use of Fourier and power series approximations.

When the problem was extended to dissipative mediums, it was shown very early [8] that waves in absorptive media exhibit finite-amplitude characteristics only at high strengths, different from waves in a non-dissipative media. More recently, an important contribution to the understanding of finite amplitude waves in a dissipative medium was presented by Fay [9]. He, similar to a later work by Blackstock [10], formulated a Fourier series solution to describe the finite-amplitude waveform for a plane wave of infinite extent. More recent theoretical approaches to finite-amplitude effects have been of two basic types: an approximation solution,

such as that proposed by Fox and Wallace [11], and a perturbation solution like that of Fay [9]. The approximation solution is based on assumed attenuation mechanisms and manner of overtone population. The perturbation solution makes use of perturbation methods and Fourier series representation of the waveform [10,12,13]. A perturbation analysis which was extended to the sixth order by Keck and Beyer [13] is of particular importance to this investigation, as will be evident later. The solution obtained by Keck and Beyer is valid near the source, unlike previous perturbation solutions of finite-amplitude traveling waves in dissipative media.

Although most investigations have been confined to traveling waves, there has been some investigations of standing waves. For example, Keller [14] extracted solutions for standing waves in a closed tube. In that investigation, Keller assumed a non-dissipative medium which resulted in infinite amplitude waves at resonance, yet still obtained useful results for frequencies close to those of resonance. Coppens and Sanders [1] developed an extension of the Keck-Beyer perturbation approach, that include wall losses as predicted by the Rayleigh-Kirchoff theory [15]. This approach was carried to the tenth order by Ruff [16], at which point it was found that the mathematics become divergent. Coppens [17] later expanded the theory and used a Fourier decomposition technique, which both Beech [3] and Winn [2] experimentally investigated. It was found that the tubes that they investigated did not behave in the manner predicted by Rayleigh-Kirchoff loss mechanisms. This investigation follows up the observation that

the tubes exhibited non-Rayleigh-Kirchoff behavior, by testing the theory using empirically determined losses.

In the theory of Coppens and Sanders, a one dimensional, non-linear wave equation with dissipative terms which correspond to those encountered in the discription of plane standing waves in a rigid-walled cavity, is developed. The wave equation in this theory can be Fourier decomposed to take the form

$$\sum_{n=1}^{\infty}\left(\frac{\partial^2}{\partial x^2} - \frac{1}{c_o^2}\,\frac{\partial^2}{\partial t^2} + D_n\right)\frac{\partial \xi_n}{\partial x} = b\,\frac{\partial^2}{\partial x^2}\left(\frac{\partial \xi}{\partial x}\right)^2 \qquad (1)$$

where

$$D_n = \delta_1\left(\frac{1}{\omega_{1r}\,n^{3/2}}\,\frac{\partial^3}{\partial x^2 \partial t} - \frac{1}{n^{\frac{1}{2}}}\,\frac{\partial^2}{\partial x^2}\right)$$

and contains a dispersive term and a dissipative term, both based on the Rayleigh-Kirchoff theory of wall losses [15], and

$\delta_1 = 1/Q_1$

ξ_n = particle displacement due to n^{th} harmonic

$\xi = \sum_n \xi_n$

$b = (1 + C_p/C_v)/2$

C_p = specific heat of medium at constant pressure

C_v = specific heat of medium at constant volume

ω_{1r} = frequency (angular) of fundamental resonance

$$Q_1 = \frac{\omega_{1r}}{\omega_{1+} - \omega_{1-}}$$

ω_{1+} and ω_{1-} are the half power frequencies above and below the fundamental.

In the description of waves in cavities, Eq. 1 can be reformulated [18] to introduce the actual cavity resonances and

generalized to include an arbitrary, empirical absorption coefficient for each mode. The result is

$$\sum_{n=1}^{\infty} K_n^2 \left[\frac{2\Delta\omega_n}{\omega_{nr}} - \frac{1}{n\omega} \frac{1}{Q_n} \frac{\partial}{\partial t} \right] \frac{\partial \xi_n}{\partial x} = b \frac{\partial^2}{\partial x^2} \left(\frac{\partial \xi}{\partial x} \right)^2$$

where

ω_{nr} = resonance frequency of the n^{th} overtone

$K_n = \frac{n\pi}{nL}$ such that pressure antinodes exist at x = 0 and at x=L

$\Delta\omega_n = n\omega - \omega_{nr}$

ω = frequency at which system is being driven, near ω_{1r}

$Q_n = \frac{\omega_{nr}}{\omega_{n+} - \omega_{n-}}$

ω_{n+} and ω_{n-} = half power frequencies above and below ω_{nr}

$$\frac{\partial \xi}{\partial x} = \frac{p}{\rho_o c_o^2} = M \sum_{n=1}^{\infty} R_n \cos K_n (L-x) \cos n(\omega t + \phi_n)$$

p = acoustic pressure

ρ_o = density of medium

C_o = thermodynamic speed of sound in medium

M = mach number

$= P_1 / \rho_o c_o^2$

P_1 = peak pressure of fundamental component of wave

R_n = Fourier coefficient of n^{th} harmonic component, normalized such that $R_1 = 1$

and

ϕ_n = phase angle of n^{th} harmonic component, where $\phi_1 = 0$.

This equation can be manipulated into a general, time-independent form which, when evaluated at the rigid boundaries of the cavity, can be further simplified to produce the following form amenable to computer calculation:

$$H_n R_n \cos(\phi_n - \theta_n) = Mb Q_1 \tfrac{1}{2} \left\{ \begin{array}{l} \tfrac{1}{2} \sum_{j=1}^{n=1} R_j R_{n-j} \cos(\phi_j + \phi_{n-j}) \\ - \sum_{j=1}^{\infty} R_{n+j} R_j \cos(\phi_{n+j} - \phi_j) \end{array} \right\}$$

and a similar form with "sin" in place of "cos",

where

$$H_n = \sqrt{\left(\frac{2\Delta\omega_n}{\omega_{nr}} Q_1\right)^2 + \left(\frac{Q_1}{Q_n}\right)^2}$$

and

$$\tan \theta_n = \frac{2\Delta\omega_n Q_1/\omega_{nr}}{Q_1/Q_n} .$$

As can be seen from the above equations, it is important to know the Q(N)'s and ω_{nr}'s of the system for the input of the theoretical predictions calculated by the computer. It is convenient to define a quantity, E(n), that indicates the position of ω_{nr} relative to the classical harmonic frequencies, $n\omega_{1r}$. E(n) is defined by

$$E(n) = (\omega_{nr}/(n\omega_{1r})) - 1.$$

The values of Q(n) and E(n) are directly determined from the infinitesimal amplitude analysis of the cavity and are the input quantities for the computer calculations.

III. EXPERIMENTAL CONSIDERATIONS

A. APPARATUS

A block diagram of the experimental apparatus is shown in Figure 1. Finite-amplitude waves were generated in air at ambient temperatures in a rectangular cavity with interior dimensions of 6.97 cm. by 20.96 cm. by 30.28 cm. The walls of the cavity were constructed of 0.985 in. thick aluminum plates, milled and screwed together to provide tight, right angle joints. These joints sealed by applying thin layers of silicon grease to adjoining surfaces before screwing them together. Acoustic waves were generated in the cavity by exciting the air with a plane-faced piston. The piston face gained access to the interior of the cavity by way of an orifice bored in one of the cavity walls. The piston was fitted with two O-rings and the piston orifice was bored such that the piston with O-rings would make an airtight fit. It was found that the piston motion was restricted by the second O-ring; therefore the piston was inserted into the orifice only as far as the first O-ring. Lubrication and further sealing of the piston-orifice interface was provided by the same high vacuum silicon grease used to seal the wall joints. The piston was attached to an M-B Electronics Model EA 1500 Exciter. This exciter was powered by two M-B Electronics Model 2120MB Power Amplifiers operating in parallel. The maximum attainable acceleration of the piston with this equipment was about 65 g's in free air at 100 Hz. The frequency and power level of the piston were controlled by a General Radio 1161-A

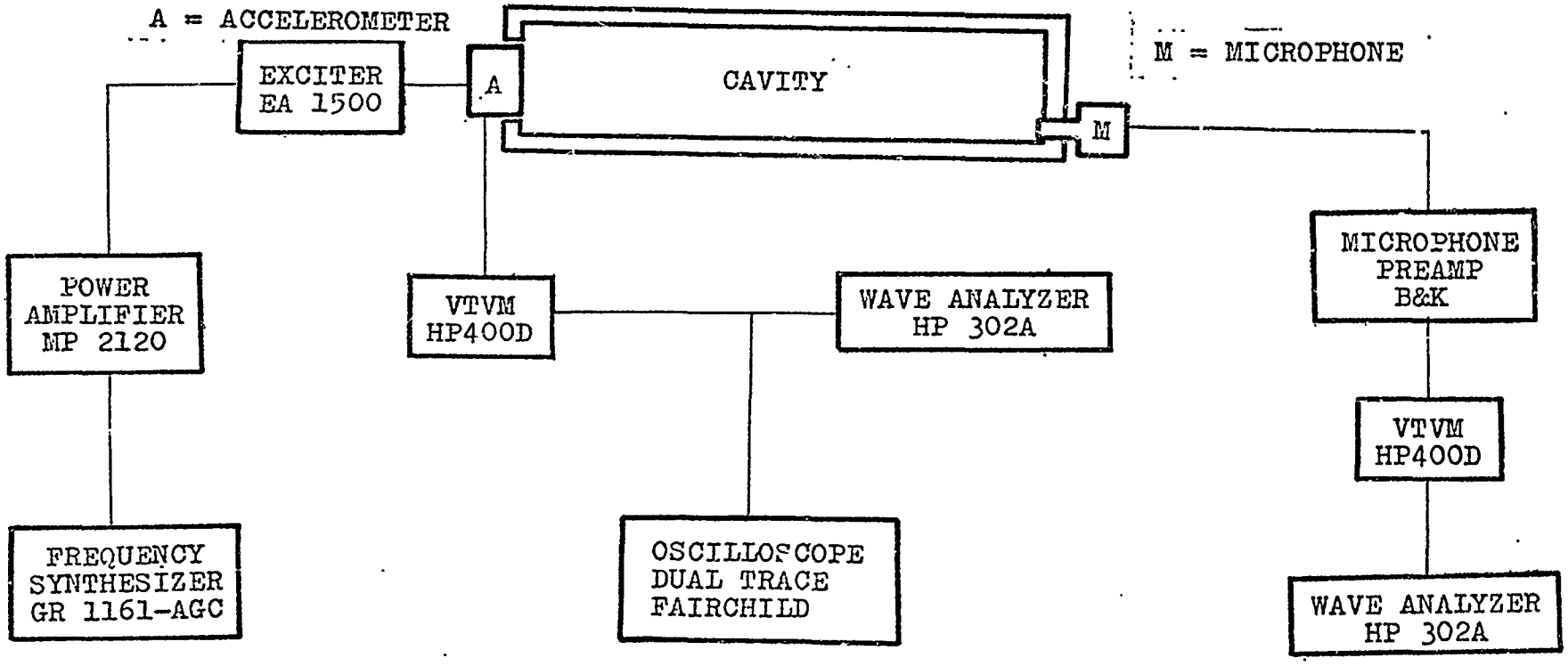

Figure 1. Apparatus

Coherent Decade Frequency Synthesizer. Frequencies can be selected to within less than 0.01 Hz with this synthesizer. The piston motion was monitored by measuring the output of an Endeveco Model 2215 Accelerometer mounted within the piston. Distortion in the piston motion, as determined by the accelerometer, set the lower limit to which reliable measurements of the non-linear distortion in the pressure waveform could be made. Measurement of the pressure waveform in the cavity was made in the far corner from the piston source. Refer to Figure 2. The sound pressure levels and harmonic components of the pressure wave in the cavity were monitored by a 1/4 inch diameter Bruel and Kjaer type 4136 Condenser Microphone. This microphone was mounted such that the active monitoring element of the microphone was flush with the interior of the cavity. The microphone was fitted with an O-ring and seated in its orifice with the same high-vacuum silicon grease. The output signal of the microphone was amplified by a Bruel and Kjaer type 2801 Power Supply. This power supply with the microphone comprized the microphone system. The microphone system was monitored by a Hewlett-Packard Model 400D Vacuum Tube Voltmeter. Another vacuum tube voltmeter of the same type was used to monitor the output of the accelerometer. A Hewlett-Packard Model 302A Wave Analyzer was used to measure harmonic distortion of both the accelerometer and microphone output signals. A Hewlett-Packard Model 521A Electronic Counter was used to monitor the filtered output of the wave analyzer to assure that the proper frequency was being analyzed.

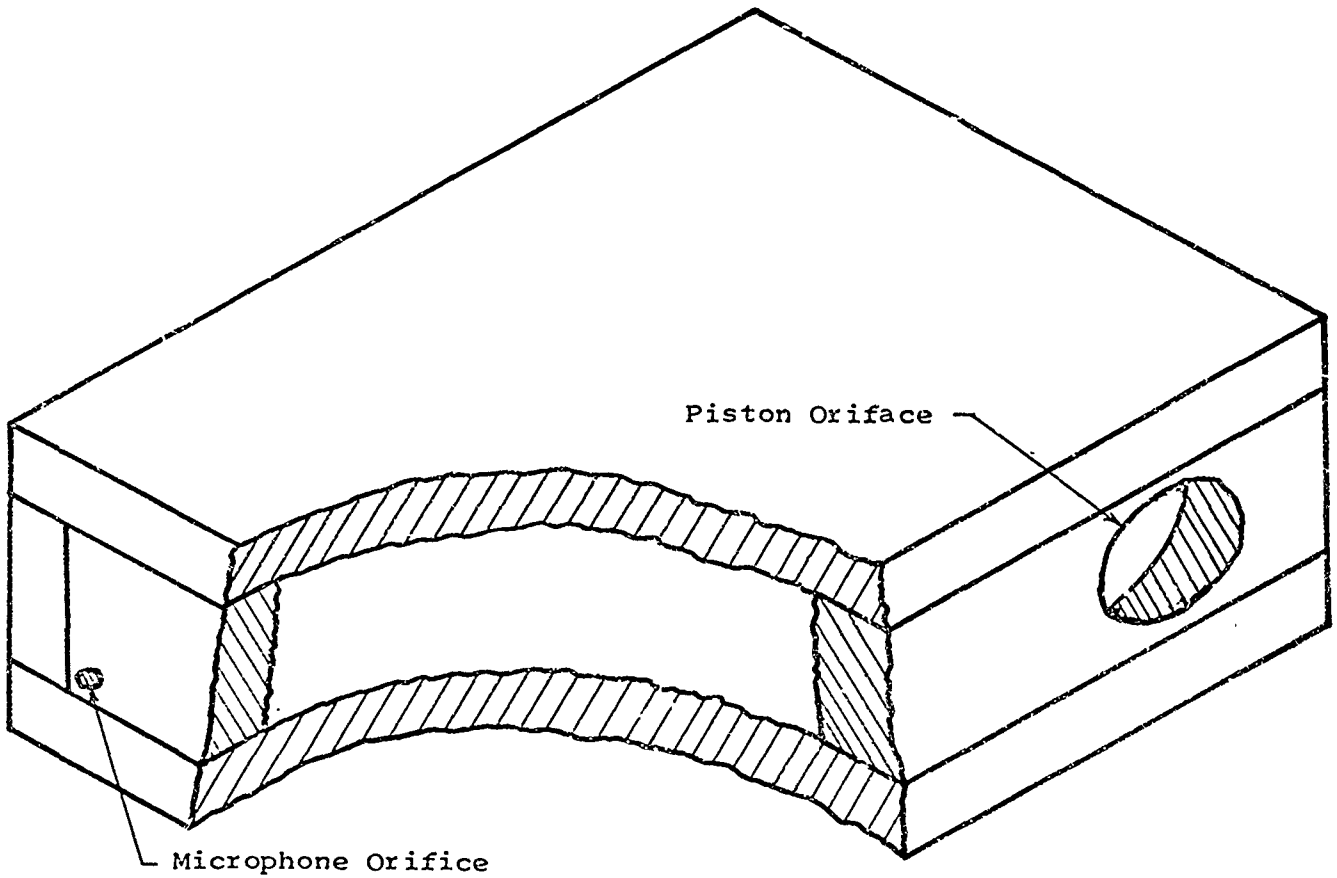

Figure 2. Rigid-Walled Cavity

B. EQUIPMENT CALIBRATION

Absolute calibration of the microphone system response was required to determine strength parameters. The microphone system included the microphone, its preamplifier, and the vacuum tube voltmeter connected to the output of the preamplifier. The microphone system response is defined by

$$S_m = V_m/P$$

where V_m is the RMS voltage from the preamplifier as indicated on the VTVM and P is the RMS pressure amplitude at the microphone face. Calibration of the microphone system was accomplished with the use of a Breul and Kjaer Model 4220 Pistonphone which produces a 124 $\pm$ 0.2 re volt/μbar acoustic signal at 250 Hz. The microphone system sensitivity was found to be

$$S_m = (1.46 \pm 0.03)\ 10^{-3}\ \text{volt}/(\text{Nt}/\text{m}^2),$$

which is in close agreement with

$$S_m = 1.50 \pm 0.03 \times 10^{-3}\ \text{Volt}/(\text{Nt}/\text{m}^2)$$

and

$$S_m = 1.52 \pm 0.03 \times 10^{-3}\ \text{Volt}/(\text{Nt}/\text{m}^2)$$

as determined by Beech [2] and Winn [3] respectively. The microphone system had a flat frequency response to within $\pm$ 0.5 db from 80 Hz. to 20 kHz., as determined from the microphone response curve supplied by the manufacturer. With the microphone system calibrated, the wave analyzers were calibrated with respect to the microphone system VTVM. This was accomplished by removing the microphone and its preamplifier from the VTVM, and substituting

a voltage signal from the frequency synthesizer to both the VTVM and the wave analyzers simultaneously.

The calibration of the accelerometer was accomplished by direct measurement of the piston face displacement at 100 Hz. and at various power settings with a stroboscopic light and a traveling microscope. The frequency of the strobe light was set very near 100 Hz so that the beats of the piston/strobe light interaction could be observed. These beats, which occur at the difference frequency $|f_{strobe} - f_{piston}|$, allowed the piston travel to be easily measurable with the traveling microscope. Twelve determinations of the accelerometer sensitivity resulted in

$$S_A = (2.36 \pm 0.04) \cdot 10^{-4} \text{ Volt}/(\text{m/sec}^2).$$

This compares with the value

$$S_A = (2.35 \pm 0.03) \cdot 10^{-4} \text{ Volt}/(\text{m/sec}^2)$$

determined by Beech [3].

C. MICROPHONE OUTPUT AND STRENGTH PARAMETER

In order to investigate the pressure waveform in the cavity, as measured at the microphone, it was necessary to relate the strength parameter to observable quantities. The strength parameter is defined as

$$SP = Mb\Omega_1.$$

The peak pressure P_1 is related to the RMS pressure P_{rms} by

$$P_1 = \sqrt{2}\, P_{rms}.$$

It is known from the microphone sensitivity that

$$P_{rms} = V/S_m$$

where V is the RMS voltage reading on the microphone system VTVM. The strength parameter can now be reformulated as

$$SP = \sqrt{2}\, VbQ_1/(S_m \rho c^2),$$

all of which are observable or calculable quantities. The calculation or measurement of each of these quantities introduces error into the determination of the strength parameter; this error is estimated to be about 1.0 to 1.5 percent for both the modes investigated.

D. FREQUENCY PARAMETER

The frequency parameter is a quantity which indicates the position of the frequency being analysed relative to the fundamental resonance of the system. The frequency parameter is defined by

$$FP = 2(\omega-\omega_{1r})Q_1/\omega_{1r}$$

and can be shown to be related to the experimental frequency increment by

$$FP = 2(\omega-\omega_{1r})/(\omega_{1+}-\omega_{1-}).$$

E. SYSTEM ALIGNMENT

The lower limit to which significant measurements could be taken was determined by the distortion introduced by the piston motion. In an effort to obtain meaningful data at the higher harmonics and for any harmonics at low strengths, great care was taken to reduce the distortion introduced into the cavity. The distortion of the piston motion when free of the cavity was below the general electronic noise level of the accelerometer system and thus was insignificant. The bulk of the distortion came from

misalignment of the piston and cavity orifice. The procedure used to obtain maximum alignment of the piston and thus minimize the distortion was as follows: The output signal of the accelerometer system, which measured the piston motion, was displayed on the dual trace oscilloscope and this waveform was compared to a pure sine wave. The piston and exciter apparatus, which was mounted in an adjustable framework, was positioned relative to the cavity orifice until the accelerometer waveform was as clean and undistorted as possible. In order to minimize any effects which may have arisen from vibration coupling of the cavity and exciter or cavity and table, the cavity was mechanically isolated from both the exciter and the table. This was accomplished by mounting both the cavity and the piston-exciter apparatus on platforms constructed of alternate slabs of wood and rubber. This restricted the interaction of the cavity with the piston to the piston orifice only. With proper alignment, it was possible to reproduce conditions where the distortion in the input waveform to the cavity was less than 0.2% second harmonic and 0.3% for third harmonic, as measured by the H-P 302A wave analyzer. Distortion values for the higher harmonics were below the general ambient noise of the total apparatus, and thus were ignored.

IV. PROCEDURES

A. PRERUN PROCEDURES

Before any meaningful data could be taken, it was important to determine the amount of vibration transferred through the cavity walls and picked up by the microphone. To make this determination, the top of the cavity was removed, thus relieving the pressure seal, and a wood plate added between the piston and microphone to isolate the microphone from the pressure waves induced in the air by the piston. As described in the System Alignment section, the cavity and the exciter-piston assemblies were isolated by a floating platform technique. The vibration picked up by the microphone was measured at frequencies of interest and produced microphone system responses of $8 \cdot 10^{-5}$ to $2 \cdot 10^{-4}$ volts. In all cases these values amounted to distortion well below 0.3%, which is the maximum amount of piston motion distortion.

It was noted by Beech [3] that temperature changes produced significant changes in the resonant frequency of the tube he investigated. The temperature effect on the cavity investigated here was very pronounced. This presented many problems as the frequency of fundamental resonance was the reference for all determinations of frequency parameter. Therefore it was necessary to know the value of the fundamental resonance at all times. To minimize this shift in the resonance frequency, the entire apparatus was allowed to warm up for a period of one to four hours, depending on the strength parameter to be investigated, prior to

taking data. This procedure did not totally relieve the effect of the frequency shift so another calibration method was employed. Many determinations of the fundamental frequency were made during the taking of data, thus producing a calibration curve, see Figure 3, by which the frequency parameter values could be corrected.

Immediately prior to the taking of each data set, the alignment of the piston and cavity was checked as outlined in the system alignment section of Experimental Considerations. From this point onward, the procedure for data collection was dictated by the quantities being measured. There was one experimental method to measure the Q's and E's of the system in the linear region, and another to measure the harmonic content of the non-linear finite amplitude waves.

B. MEASUREMENT OF Q(N) AND E(N) IN THE LINEAR REGION

Data collection in this region required very little power, but required very fine control of the power setting. This control was obtained by inserting a voltage dividing circuit between the frequency synthesizer and the power amplifiers. This voltage divider reduced the available power by a factor of ten and increased the sensitivity of the power control by the same factor of ten. With this arrangement, a satisfactory fine tuning power control was obtained at low strengths.

With the power set at some nominal low value, the frequency region about the resonant or harmonic pressure peak of interest was scanned until a maximum in pressure was indicated by the

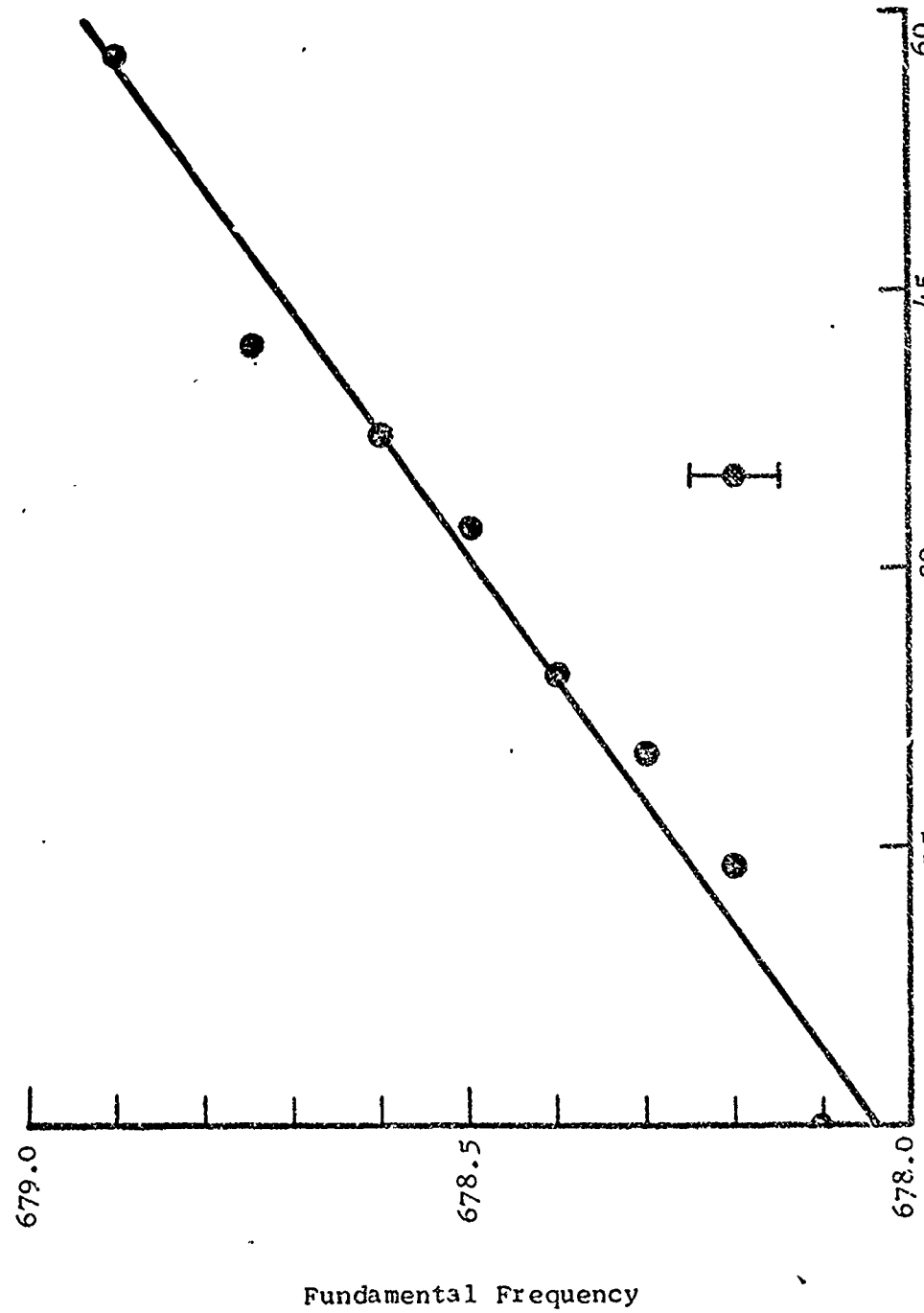

Figure 3. Fundamental Frequency Calibration Curve

microphone system response. The input power, determined in the linear, low strength, region, and kept constant during the following measurements. The frequency of the driving piston was changed above and below the frequency of maximum pressure, until the pressure was -3 dB of the maximum pressure value. This determination of the -3 dB points was made with the 302A wave analyzer, which measured the pressure amplitude of the cavity by way of the microphone system.

It was found that the first seven overtones of the n00 mode and the first five overtones for the 0n0 mode were undisturbed by overlapping Q curves. The value of Q for each response curve was determined from the frequency difference of the -3 dB points, divided by the center point frequency between the two -3 dB points. This center point was assumed to be a good estimate of the peak pressure frequency, ω_{nr}, for the response curve in question. It was with these values for the system resonance frequencies that the E(n)'s were determined.

C. MEASUREMENT OF THE HARMONIC CONTENT OF FINITE AMPLITUDE STANDING WAVES

In order to obtain finite amplitude waves in the cavity, it was necessary to go to much higher strengths than were required for the measurement of the Q's and E's. With the driving frequency set to some value near the fundamental, and the peak pressure component of the fundamental held constant, the strength of each harmonic was measured by one of the wave analyzers. The other wave analyzer monitored the fundamental pressure P_1, which

was kept constant by varying the power setting of the synthesizer as necessary. Values of the frequency parameter were chosen such that the distortion curves, Figures 4 through 9, could be determined in the areas of maximum distortion. The order in which measurements were taken for each distortion curve was randomized to avoid systematic error. Strength parameters of about 0.5, 0.75, and 1.0 were investigated for each mode. Strengths below 0.5 did not produce high enough distortion to be measured with the equipment available. Strengths above 1.0 were not accessable due to limitations in power.

V. RESULTS

Tables I and II are the data for the linear, infinitesimal amplitude region. The information on the empirical losses is contained in the Q's and E's. These are the values used in the computer program to predict the harmonic distortion curves in Figures 4 through 9. The theoretical curves in these figures are plotted along with the experimentally measured values of harmonic distortion. The theoretical predicted values were generated for frequency parameter intervals of 0.2 and were plotted as solid curves. The experimentally measured values were plotted as dots where they occured. Data were taken, and theoretical predictions made, for strength parameters of 0.513, 0.782, and 1.00 for the n00 mode and 0.507, 0.780, and 1.00 for the 0n0 mode.

The point of intersection of the error bars on the P_2/P_1 theoretical curve in Figure 4 corresponds to the value of $EP = 2Q_1E(2)$ where $\omega = \frac{\omega_{2r}}{2}$. It is important to note that the n = 2 distortion curves peak when the system is driven at this frequency. That is, when the driving frequency ω is equal to the classical fundamental of ω_{2r}, there is maximum content of P_2. The point where this occurs for each P_2/P_1 curve is indicated by arrows in Figures 5 through 9 and by crossed error bars in Figure 4. The error in the determination of these points comes mainly from the error in E(2) that appears in the above equation for EP. The error in Q_1 is of much less significance as is indicated in Table III. The error in the P_2/P_1 curves in Figures 5 through 9 are approximately the same as those indicated in Figure 4.

Table 1

nOO Mode

n	f_-(Hz)	f_+(Hz)	Δf(Hz)	f_n(Hz)	Q	E x 10^3
1	677.80	679.70	1.90	678.75	357.24	0
2	1365.74	1368.49	2.75	1367.12	497.13	7.0
3	2059.17	2062.84	3.67	2061.01	561.58	12.0
4	2787.37	2792.73	5.36	2790.05	520.53	27.5
5	3423.00	3427.80	4.80	3425.40	713.63	9.1
6	4126.41	4131.91	5.50	4129.16	750.76	13.6
7	4803.92	4809.93	6.01	4806.93	799.82	11.4
1	678.02	679.95	1.93	678.99	351.81	0

Table II

OnO Mode

n	f_-(Hz)	f_+(Hz)	Δf(Hz)	f_n(Hz)	Q	E x 10^3
1	813.99	816.08	2.09	815.04	389.97	0
2	1633.16	1636.39	3.23	1634.78	506.12	2.8
3	2415.11	2420.57	5.46	2417.84	442.[illegible]	-11.3
4	3143.74	3150.10	6.36	3146.92	494.80	-34.9
5	3911.05	3920.35	9.30	3915.70	423.62	-39.4
1	814.23	816.34	2.11	815.29	386.39	0

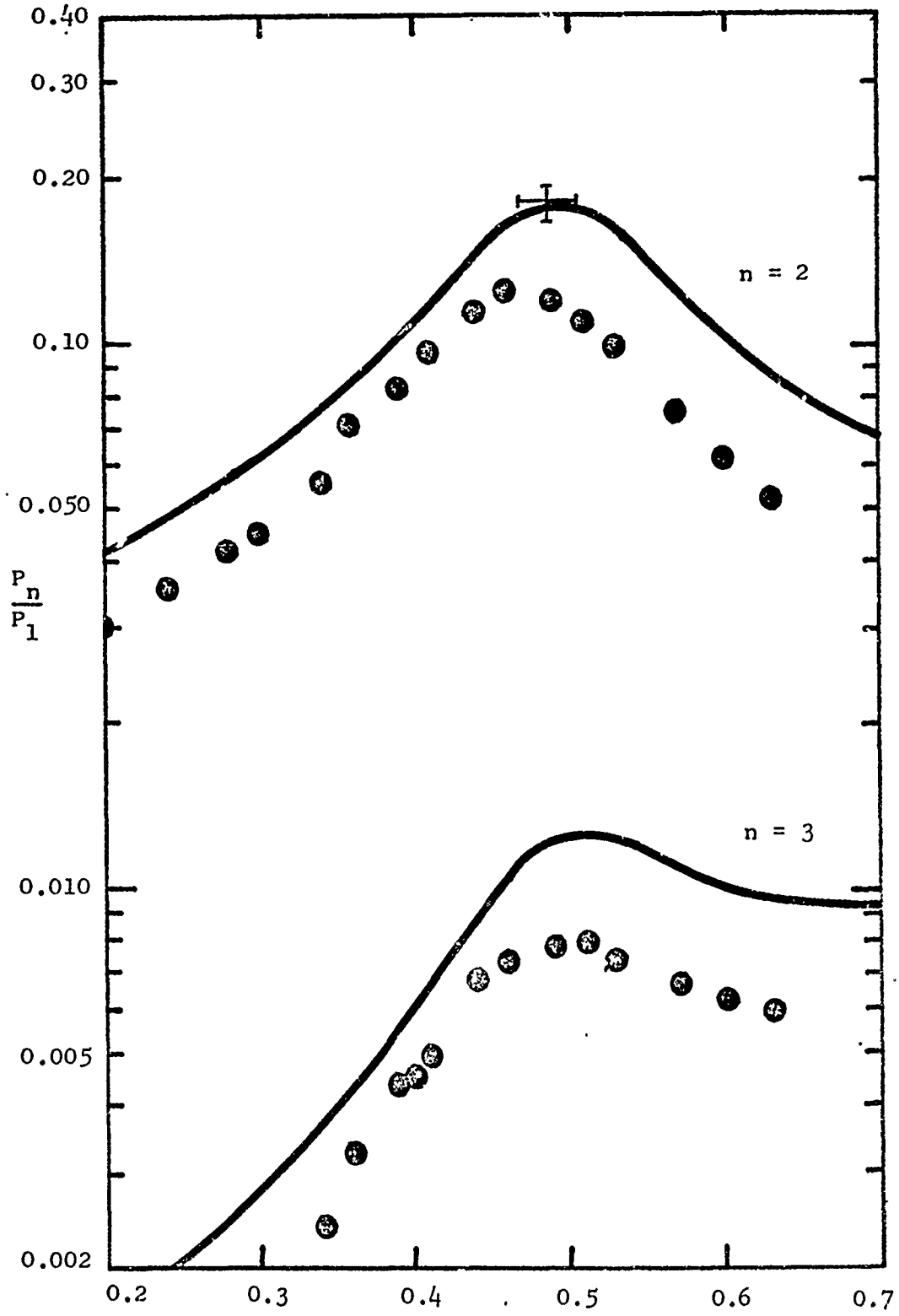

n00 Mode SP = 0.513

Figure 4

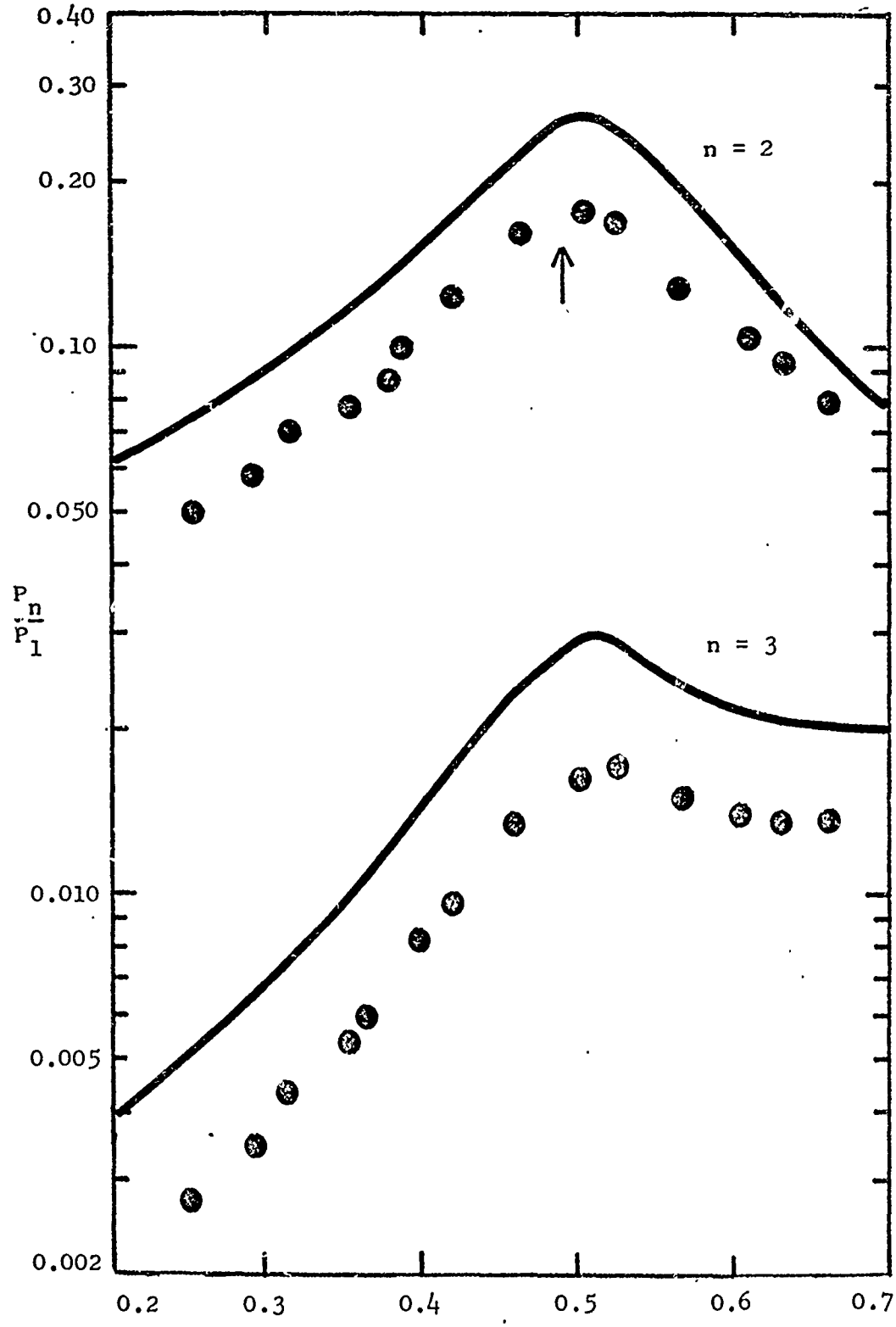

n00 Mode SP = 0.782

Figure 5

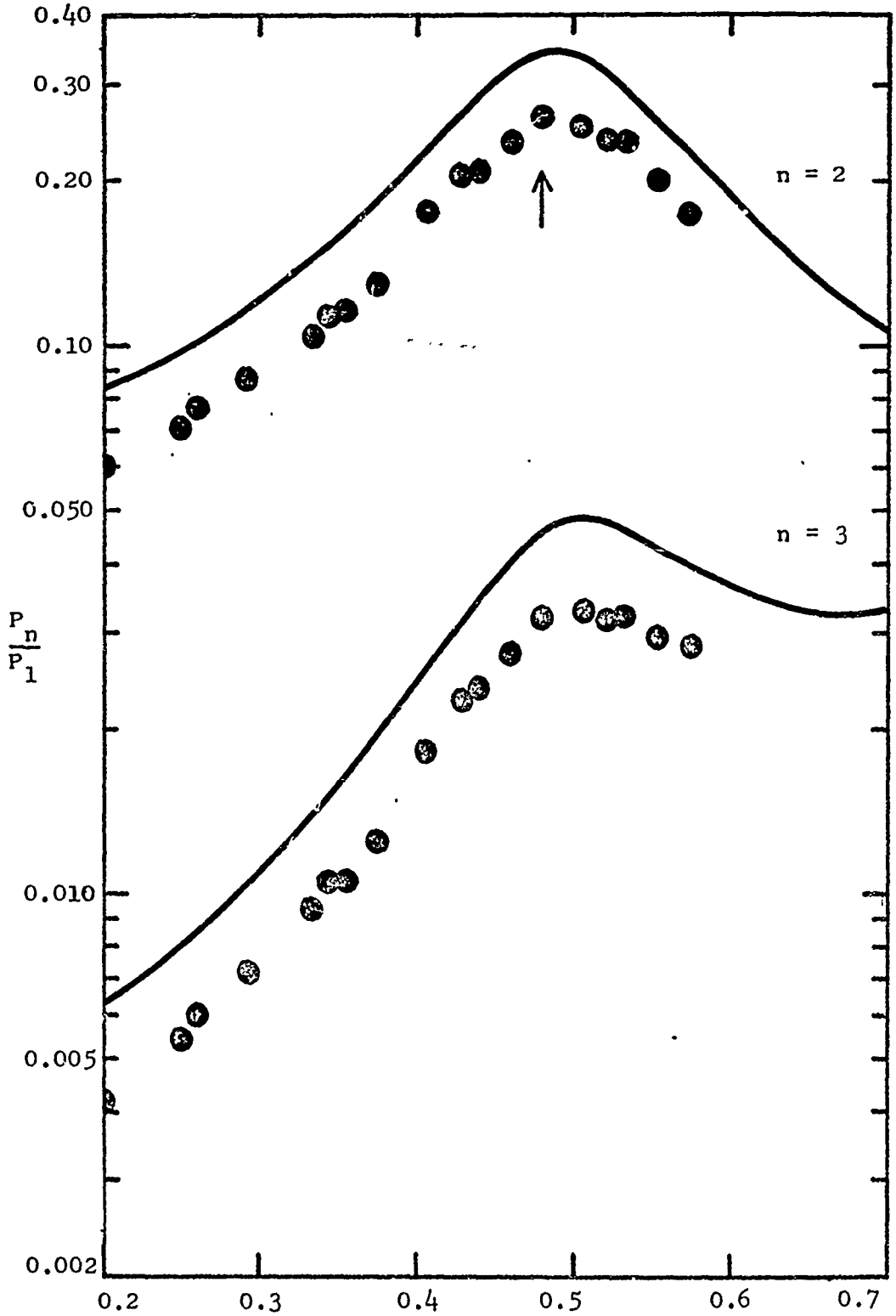

n00 Mode SP = 1.00

Figure 6

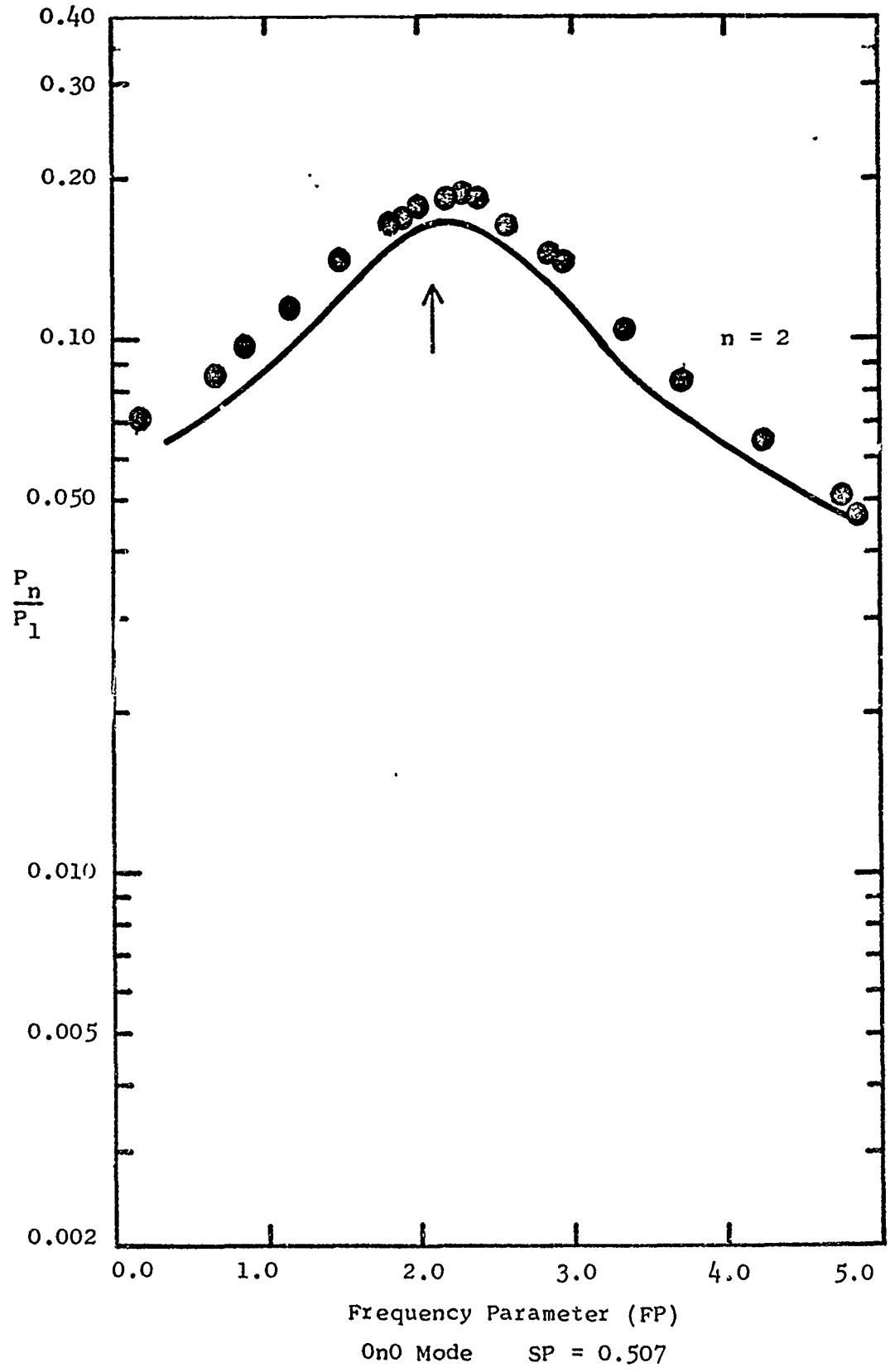
0.40
0.30
0.20
0.10
0.050
0.010
0.005
0.002
$\frac{P_n}{P_1}$
n = 2
0.0
1.0
2.0
3.0
4.0
5.0
Frequency Parameter (FP)
0n0 Mode SP = 0.507

Figure 7

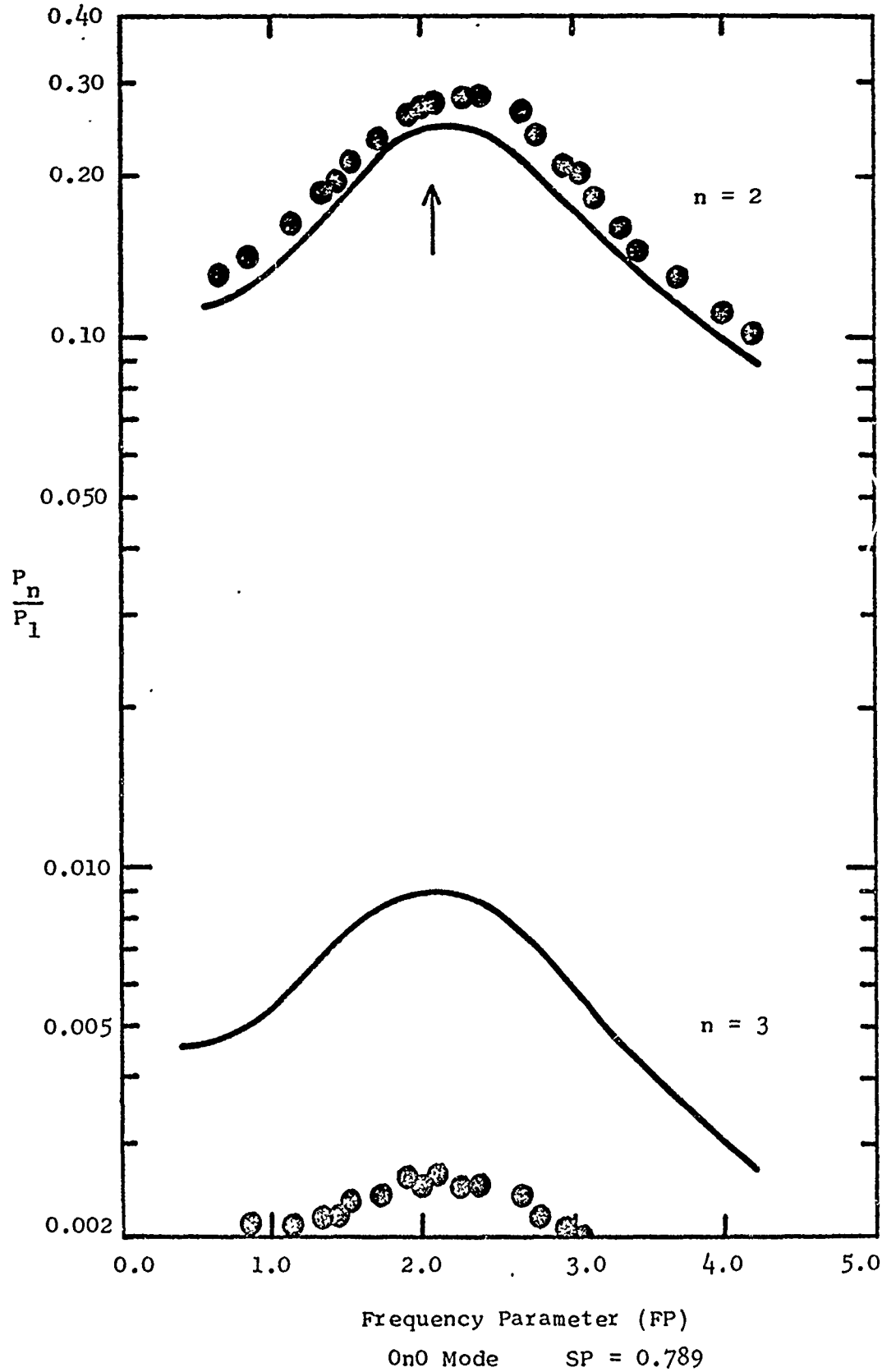
0.40
0.30
0.20
0.10
0.050
0.010
0.005
0.002
$\frac{P_n}{P_1}$
n = 2
n = 3
0.0
1.0
2.0
3.0
4.0
5.0
Frequency Parameter (FP)
0n0 Mode SP = 0.789

Figure 8

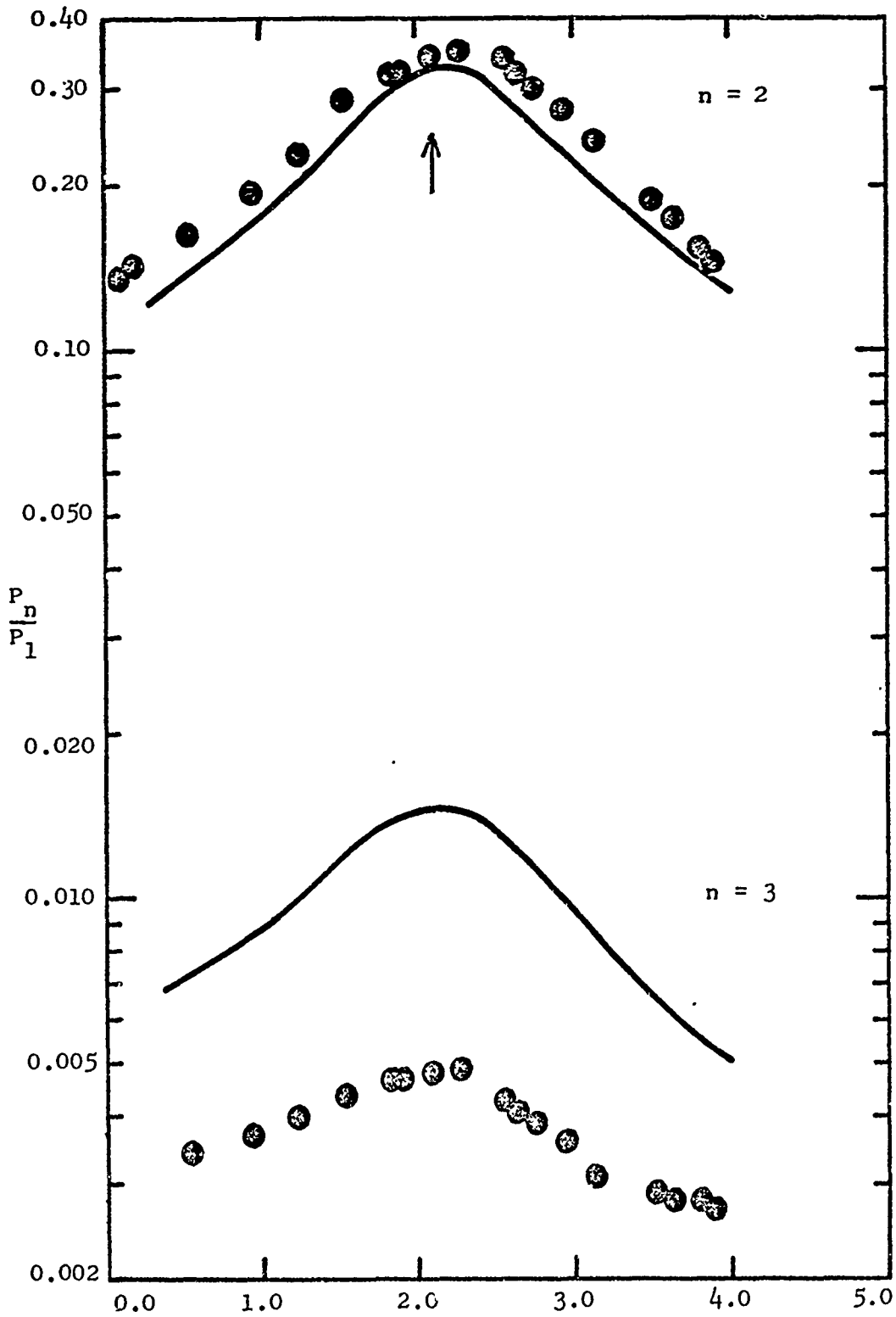

OnO Mode SP = 1.00

Figure 9

Table III contains the results of five separate determinations of the Q's and E's taken in the infinitesimal amplitude region. These measurements were made to provide an estimate of the error in the theoretical curves. In all cases the values used to generate the curves were very close to the average values determined later and the regeneration of the curves was therefore unwarranted. Table III contains both sets of values for direct comparison.

Table III

n00 Mode

	Average Values		Values Used to Determine Curves	
n	Q(n)	$E(n)\cdot 10^3$	Q(n)	$E(n)\cdot 10^3$
1	358.2 ± 0.4	-----	357.2	-----
2	498.5 ± 4.7	6.8 ± 0.1	497.1	7.0
3	559.8 ± 0.8	11.6 ± 0.2	561.6	12.0
0n0 Mode				
1	359.8 ± 5.3	-----	390.0	-----
2	515.7 ± 5.1	2.6 ± 0.1	509.1	2.8
3	459.2 ± 7.5	-11.3 ± 0.1	442.8	-11.3

VI. CONCLUSIONS

It appears that the present theoretical model successfully predicts the major features of the harmonic content for finite-amplitude standing waves in a rigid-walled cavity. In all cases investigated, the shape and general magnitude were predicted; see Figures 4 through 9.

It is interesting to note the position of each theoretical curve relative to its corresponding experimental curve. For the n00 mode, the theoretically predicted values are consistently above the measured values. The situation for the 0n0 mode is the same for P_3/P_1 but opposite for P_2/P_1. A possible source of this difference is the large difference in the geometry encountered by each mode. The n00 mode is a standing wave whose wave vector is perpendicular to the wall with the microphone orifice, which must be considered a very small perturbation due to its small size. On the other hand, the 0n0 mode is a standing wave with its wave vector perpendicular to the piston orifice, which is a large perturbation in the geometry. In addition, the fact that the wave generating surface, the piston face, is normal to the n00 wave vector and perpendicular to the 0n0 vector could cause a consistant difference in the behavior of the modes. It is certainly unclear to this investigator just what the specifics are that explain the trends in the theory/experiment relationship. It is clear however, that the theory of Coppens and Sanders as modified to include empirical losses, does predict the essence of the

behavior of finite-amplitude standing waves in the rigid-walled cavity investigated.

APPENDIX A

In the investigation by Winn [2], it was found that the tubes analyzed did not behave in a manner consistent with Rayleigh-Kirchoff wall losses. In an effort to determine if the interior finish of the tubes was a critical factor that determined the loss mechanisms, the six foot tube was reanalyzed after refinishing the interior to a highly polished state. These results were compared to the results for the tube in a smooth but not polished condition as determined by Winn.

It was found that the absorption coefficients, defined as

$$\alpha_n = \frac{\omega_{n+} - \omega_{n-}}{2C_o} ,$$

were not significantly changed from the values found by Winn, and both sets of values obeyed the Rayleigh-Kirchoff predictions indicated by the solid line in Figure 10. The behavior of the overtones (for the polished tube) was found to be significantly different (from the overtone behavior in the unpolished tube), and was significantly different from the Rayleigh-Kirchoff predictions as indicated by a solid line in Figure 11.

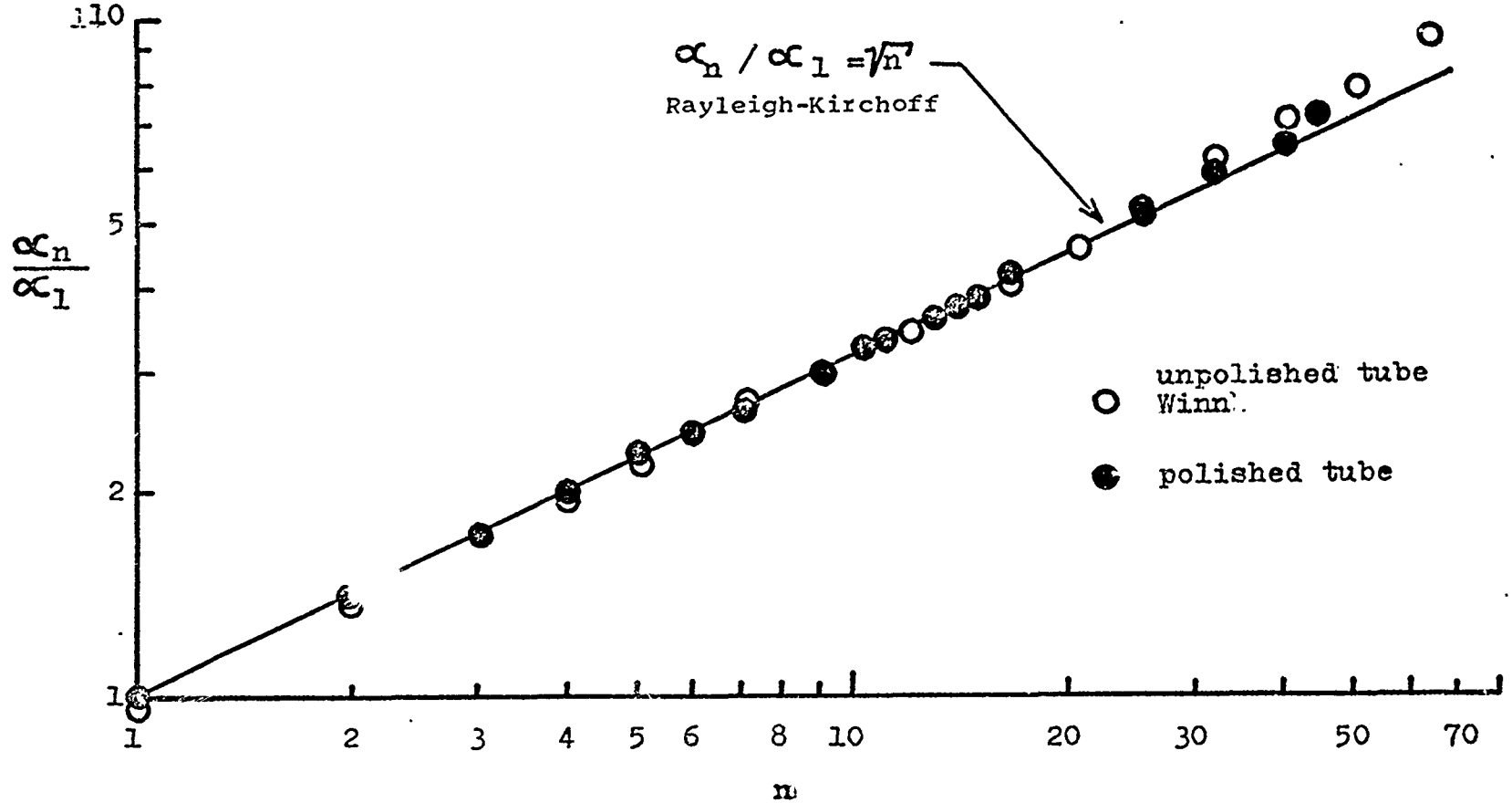

Figure 10. Comparison of Attenuation Coefficients

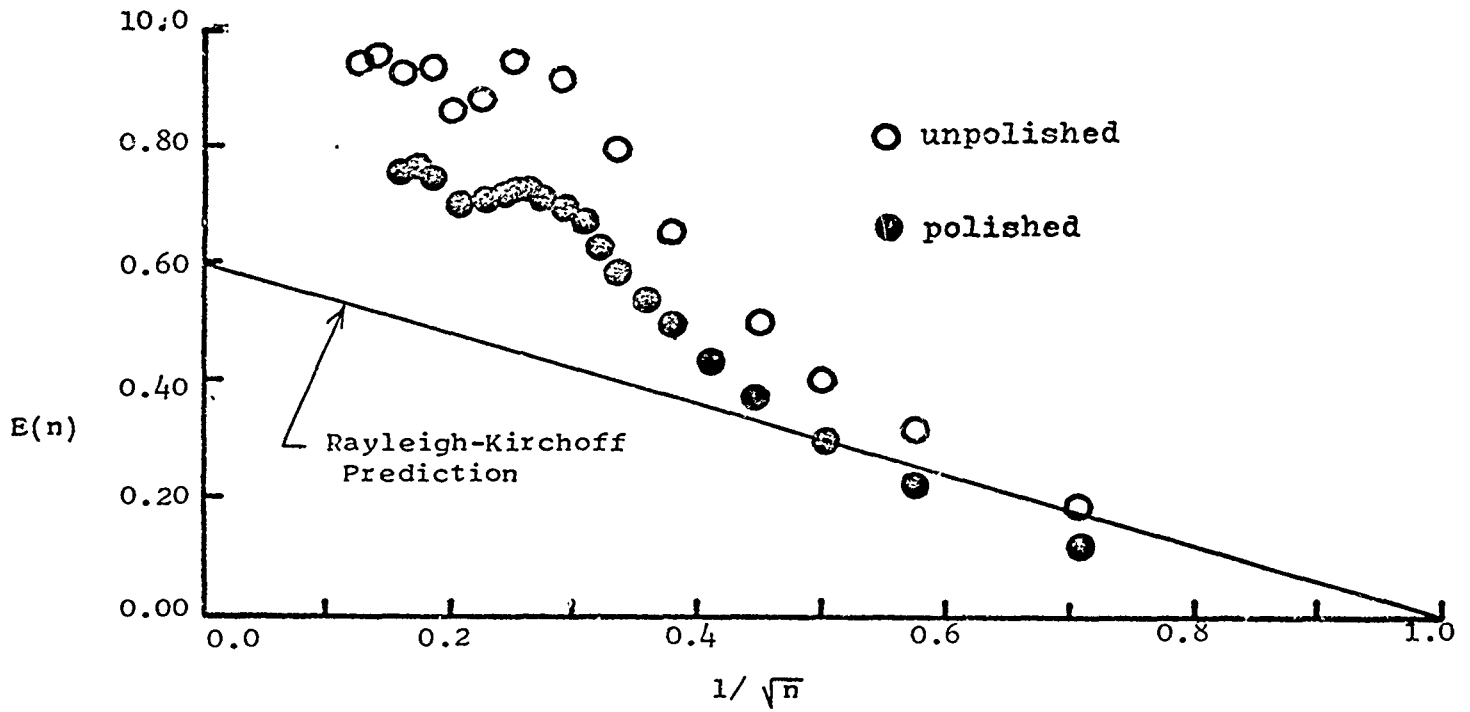

Figure 11. Comparison of E(n)s

BIBLIOGRAPHY

1. Coppens, A.B., and Sanders, J.V., "Finite-amplitude Standing Waves in Rigid Walled Tubes," J. Acoust. Soc. Am., V. 43, P. 516-529, March 1968.

2. Winn, J.R., Fourier Analysis of Experimental Finite-amplitude Standing Waves, Thesis, Naval Postgraduate School, Monterey, California, 1971.

3. Beech, W.L., Finite-amplitude Standing Waves in Rigid-walled Tubes, Thesis, Naval Postgraduate School, Monterey, California, 1967.

4. Kirchoff, G., Ann. Phys. Leipzig, V. 134, P. 177-193, 1868.

5. Lamb, H., Dynamical Theory of Sound, 2d ed., Chap. VI, Edward Arnold and Co., London England, 1925.

6. Fay, R.D., "Successful Method of Attack on Progressive Finite Waves," J. Acoust. Soc. Am., V. 28, P. 910-914, September 1956.

7. Blackstock, D.T., "Propagation of Plane Sound Waves of Finite Amplitude in Nondissipative Fluids," J. Acoust. Soc. Am., V. 34, P. 9-30, January 1962.

8. Lord Rayleigh, Theory of Sound, 2d ed., V. 1 and 2, Dover Publications, Inc., New York, 1945.

9. Fay, R.D., "Plane Sound Waves of Finite Amplitude," J. Acoust. Soc. Am., V. 3, P. 222-241, 1931.

10. Blackstock, D.T., "Convergence of the Keck-Beyer Perturbation Solution for Plane Waves of Finite Amplitude in a Viscous Fluid," J. Acoust. Soc. Am., V. 39, P. 411-413, 1966.

11. Fox, F.E., and Wallace, W.A., "Absorption of Finite Amplitude Sound Waves," J. Acoust. Soc. Am., V. 26, P. 994-1006, 1956.

12. Gol'berg, Z.A., Akust. Zhur. V. 3, P. 149, 1957, (English Trans.; Sov. Phys. - Acoust. V. 3, P. 157, 1957).

13. Keck, W., and Beyer, R.T., "Frequency Spectrum of Finite Amplitude Ultrasonic Waves in Liquids," Phys. Fluids, V. 3, P. 346-352, 1960.

14. Keller, J.B., "Finite Amplitude Sound Produced by a Piston in a Closed Tube," J. Acoust. Soc. Am., V. 26, P. 253-254, 1954.

15. Weston, D.E., Proc. Phys. Soc., (London) B66, 695-709, 1953.

16. Ruff, P.G., Finite Amplitude Standing Waves in Rigid Walled Cavities, Thesis, Naval Postgraduate School, Monterey, California, 1967.

17. Coppens, A.B., "Theoretical Study of Finite-Amplitude Traveling Waves in Rigid-Walled Ducts: Behavior for Strengths Precluding Shock Formation." J. Acoust. Soc. Am., V. 49, P. 306-318, 1969.

18. Coppens, A.B., personal communication.